Appl. Phys. B 51, 53–58 (1990)

Applied Physics B Photophysics and Laser Chemistry

The Impact of Laser Field Statistics in Determination of Temperature and Concentration by Multiplex USED CARS

B. Lange and J. Wolfrum

Physikalisch-Chemisches Institut der Universität, Im Neuenheimer Feld 253, D-6900 Heidelberg, Fed. Rep. Germany

Received 21 December 1989/Accepted 7 February 1990

Abstract. Experiments have been performed which demonstrate that the ratio of resonant to nonresonant third-order susceptibilities measured in multiplex USED CARS are affected by the time correlation of the pump fields. Comparing the resonant to nonresonant signal ratio obtained with decorrelated fields to the ratio obtained with correlated fields, a relative increase of 2.5 was measured for the nitrogen Q-branch, whereas a corresponding increase of 1.9 was observed for the hydrogen $Q(1)$-line. To compare our experimental results with theoretical calculations of the spectral shapes, the nonresonant third-order susceptibilities of a number of gases were re-evaluated by calibrating to the nonresonant susceptibility of argon.

PACS: 42.65Dr

Coherent anti-Stokes Raman scattering (CARS) is a spectroscopic technique which allows instantaneous measurements of temperature and species concentration. High and collimated signal intensity generated by short and ultrashort laser pulses and a high spatial resolution of tenths of a mm^3, in conjunction with an anti-Stokes shifted signal wavelength has enabled the application of CARS even in industrial environments [1]. The ultimate goal in CARS is to derive temperature and concentration of various molecules simultaneously, either from spectral shape or from absolute signal intensity [2, 3]. The results of such measurements are in general as precise as the theoretical modelling of the experimental spectrum.

During the past decade, progress in modelling CARS-spectra was achieved by incorporating effects like collisional narrowing [4] and cross coherence [5, 6]. Among other processes, a potential source of measurement errors was found in the use of time-correlated multimode pump laser beams in crossed, phase-matched beam configurations [7]. In this contribution it is shown how laser field statistics affect the determination of temperature and concentration in multiplex USED CARS [1] applications.

USED CARS is especially suitable when pump laser beams originating from diffractively-coupled unstable resonators are employed. Its insensitivity to beam steering, its high signal intensity with relatively high spatial resolution and ease of alignment are advantages of this technique. Moreover, the beam setup in USED CARS satisfies simultaneously the phase matching condition for a large pressure range [8]. The measurements reported were performed using a broadband CARS spectrometer. This avoids the need of an additional reference channel, as usually employed in narrowband CARS [7], because of the short measurement times and high repetition rates [9].

The measurements reported were performed in calibrated binary mixtures of resonant and nonresonant gases. CARS spectra were obtained with correlated and uncorrelated pump fields in a USED CARS configuration as well as with decorrelated pump fields in a BOXCARS [1] setup. Multiplex CARS spectra were obtained from mixtures of hydrogen/nitrogen and nitrogen/oxygen as the resonant/nonresonant species. Spectra of the latter mixture were compared with theoretical calculations. In addition, pure resonant and nonresonant signal intensities were meas-

ured. For calibration purposes a number of effective nonresonant susceptibilities were re-evaluated.

1. Theory

When phase-matching requirements are satisfied, a CARS signal at frequency $\omega=\omega_1+\omega_3-\omega_2$ is generated by the interaction of two photons of frequency ω_1 and ω_3 (usually termed pump photons and, in the following, frequency degenerate, $\omega_1=\omega_3$) with a photon of frequency ω_2 (termed Stokes photon) via the third-order susceptibility $\chi^{(3)}(\omega,\omega_1,-\omega_2,\omega_1)$ of the medium. The CARS intensity is given by the $K-T$-formalism [5, 6] as:

$$I(\omega)=\chi_{NR}^2\langle 1\rangle+2\chi_{NR}\langle \mathrm{Re}\{\chi_R(\omega-\omega')\}\rangle + 1/2\langle|\chi_R(\omega-\omega')|^2\rangle + 1/2\langle\chi_R(\omega-\omega')\chi_R^*(\omega-\omega'')\rangle \quad (1)$$

$$\langle F\rangle=\int d\omega' I_1(\omega')\int d\omega'' I_1(\omega'')F(\omega',\omega''),$$

where χ_R denotes the resonant third-order susceptibility, χ_{NR} the effective nonresonant third-order susceptibility and $I_1(\omega)$ the spectral distribution of the pump laser [10]. In deriving (1), the Stokes laser integration was neglected because in multiplex CARS, the Stokes intensity distribution is usually much broader than the pump laser distribution. Consequently, measured spectra are referenced by spectra of a purely nonresonant gas.

For crossed, linearly polarized laser beams, the third-order susceptibility of a gaseous medium in terms of the tensor components of $\chi^{(3)}(\omega)$ can be expressed as [11]:

$$\chi^{(3)}(\omega)=\chi_R(\omega)+\chi_{NR}=3\chi_{1111}(\omega)\phi(\varrho) + (\chi_{NR,r}+\chi_{NR,b})\phi(1/3). \quad (2)$$

Here, subscripts r and b denote the resonant and buffer gas species, respectively, ϕ is given by $\cos\alpha\cos\beta+\varrho\sin\alpha\sin\beta$, where α and β are the angles between polarization of pump and Stokes beams and pump beam and analyzer, respectively (if no analyzer is used $\beta=0$) and ϱ the depolarization ratio of the Raman resonant molecule. Off-resonant Raman contributions of the buffer gas are included in $\chi_{NR,b}$. The tensor-component $\chi_{1111}(\omega)$ can be written as:

$$3\chi_{1111}(\omega)=(2\pi N/h)\boldsymbol{\alpha}\cdot\mathbf{G}(\omega)^{-1}\cdot\mathbf{p}\cdot\boldsymbol{\alpha} \quad (3)$$

where N is the absolute number density of Raman resonant molecules, $\boldsymbol{\alpha}$ a vector of transition amplitudes, $\mathbf{p}$ a diagonal matrix of fractional population differences and $\mathbf{G}(\omega)$ the relaxation matrix. The other symbols have their usual meaning. Further details of the calculation algorithms can be found in [12, 13].

From (2) and (3) it follows that – especially at high temperatures and low concentration of Raman resonant molecules – an enhancement of the nonresonant signal contribution due to laser field statistics can result in systematic errors in derived temperature and concentration.

The origin of the enhancement can be better understood by studying the molecular response to the applied external electrical fields of pump and Stokes laser. The external electromagnetic fields act as a driving force in the medium. Due to its relatively high mass the nucleus of a molecule cannot follow the rapid amplitude fluctuations of a multimode pump-laser field as fast as the electronic contributions (which are summed up to χ_{NR}) do. However, for Gaussian statistics of the pump field fluctuations, resonant and nonresonant intensities increase in a similar manner. As a consequence, for Gaussian statistics, the ratio of resonant to nonresonant CARS intensities is nearly independent of the coherence between intensity fluctuations of the pump beams [7]. Decorrelated pump fields are given when the relative delay between the two pump beams amounts to several times the coherence length which can be calculated from the pump laser linewidth. For non-Gaussian pump laser field statistics, an enhancement of the ratio ε – given by resonant to nonresonant intensities of decorrelated relative to correlated pump fields – generally occurs, as long as the Raman relaxation time T_2 is long compared to the typical time τ_c of intensity fluctuations in the pump field. Decorrelated pump laser fields exist provided $\delta\gg\max(T_2,\tau_c)$.

Using a simplified model to describe the amplitude fluctuations following Gaussian statistics, it has been shown that ε can be calculated as a function of relative delay δ between the pump laser fields using the first- and higher-order correlation functions [7]. More detailed expressions, including non-Gaussian [14] and super-Gaussian laser field statistics have been derived [15]. A further approach [16] gives an expression for the nonresonant signal increase as a function of doubling efficiency of the fundamental Nd : YAG-laser beam at 1.064 µm and describes effects of non-Gaussian pump field fluctuations as non-thermal cross coherence [17]. However, it seems to be more reliable and easier to achieve uncorrelated pump laser fields experimentally than to incorporate these theoretical models in CARS-fitting codes.

2. Experimental Setup

The broadband CARS spectrometer is shown schematically in Fig. 1 in a folded BOXCARS setup. The USED CARS setup has been described previously [8, 18] when temperature and concentration profiles of a laminar counterflow diffusion flame were obtained. In Ref. [18] the nonresonant signal contribution was

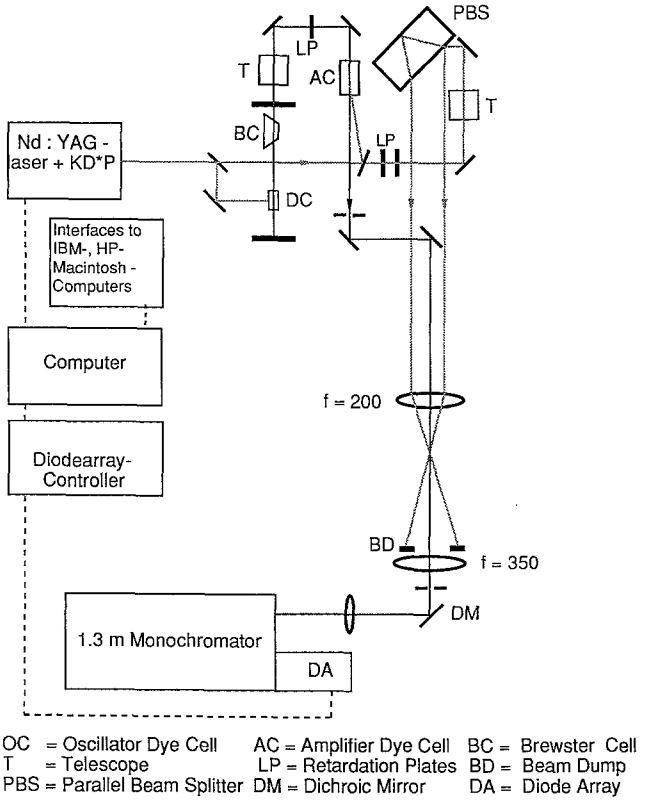

Fig. 1. Broadband CARS spectrometer in BOXCARS setup

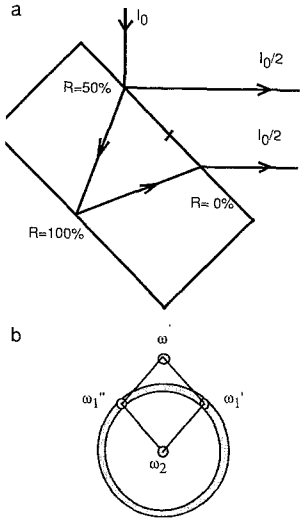

Fig. 2. a Beam splitter for equally strong and decorrelated BOXCARS pump beams. **b** Schematic diagram of USED CARS as circular rotated BOXCARS

suppressed by polarization techniques, ruling out measurement errors caused by an enhancement of nonresonant signal contributions.

The frequency doubled donut-shaped output of a Nd:YAG-laser (100 mJ, linewidth 0.8 cm^{-1} FWHM, pulse duration 8 ns) acts as the pump beam in the CARS process as well as pumping a home-made broadband dye laser. The dye laser was operated with pyridine dissolved in methanol to match the hydrogen Q-branch at 4155 cm^{-1} ($\lambda_s = 683$ nm) and rhodamine 101 for the nitrogen Q-branch at 2330 cm^{-1} ($\lambda_s = 607$ nm), respectively. The bandwidth of the Stokes laser was narrowed by an intracavity etalon to 50 cm^{-1}. By angle-tuning the etalon, the Stokes intensity maximum can easily be shifted spectrally. In addition, possible off-resonant contributions are avoided by such a narrow Stokes source.

The polarizations of pump and Stokes beams were made linear and parallel by means of retardation plates and polarizers. In USED CARS, the circular pump beam was enlarged to a diameter of 18 mm. To a large extent, decorrelated pump fields were created by means of two square rods of quartz. After being combined, coaxial pump and Stokes beams were focused by an $f = 200$ mm achromatic lens into a cell equipped with sealed quartz windows. 23 mJ pump energy and 5 mJ (H_2) or 11 mJ (N_2) Stokes energy were applied. The cell pressure was measured by two capacity manometers (MKS Baratron) for the pressure ranges up to 10 and 800 Torr, respectively. BOXCARS measurements were performed by reducing the circular pump beam to a diameter of 3 mm and by means of the beam splitter shown in Fig. 2a. Thickness and refractive index were chosen to produce a horizontal distance of 13.5 mm and a path delay of the equally strong pump beams of 46 mm, which is nearly three times the coherence length (16 mm). In addition, this type of beam splitter eliminates the sometimes difficult alignment of the pump beams because here they are automatically parallel to one another. The same amount of energy and the same focusing lens were used in the BOXCARS experiments. In Fig. 2b it is also shown how the USED CARS process can be thought of as the sum of single BOXCARS scattering events. USED CARS signals were spectrally filtered by using a short-wave pass and a dichroic mirror. BOXCARS signals were filtered spatially by an aperture and spectrally by a dichroic mirror. After passing through a 1.3 m-monochromator (McPherson Mod 209, equipped with a 2400 l/mm grating) signals were detected by a linear diode array (SI, IRY 512). From a fit of CARS flame spectra, the dispersion at the nitrogen CARS wavelength of 473 nm was found to be 0.00266 nm per pixel and the overall spectral resolution from room air spectra to be 0.009 nm. The BOXCARS interaction volume was measured to be 1.1 mm × 80 μm (L_{95}). Performing the USED CARS measurements and carefully adjusting identical foci of pump and Stokes laser beams, we obtained strong biharmonic pumping [19] at a pump energy as low as 10 mJ and a Stokes energy of 9 mJ, respectively. The vibrational temperature derived from the laser stimulated population of the higher vibra-

tional states amounts to 2620 K, measured in ambient room air. The rotational temperature of the ground and first vibrational states remained constant at 300 K. By slightly defocussing the Stokes laser, biharmonic pumping was reduced until no vibrational hot band could be observed at room temperature. The resonant signal BOXCARS intensity in ambient room air was of the order of 6×10^6 detector counts per laser pulse (inserting a sheet of white paper in front of the entrance slit, the signal could be seen by eye). A correction of the detected signal intensities due to the measured nonlinear response of the diode array was not significant because the signal strength was set by calibrated neutral density filters to be in the range of linear detector gain. Measured spectra were stored and referenced by a laboratory computer and subsequently transferred to an IBM 3090-180 mainframe.

3. Results and Discussion

In the pressure range studied here the impact of laser field statistics is related mainly to the intensity associated with the nonresonant third-order susceptibility χ_{NR}. Therefore we decided first to re-evaluate χ_{NR} for a number of gases. This was done by comparing the absolute intensities and the intensity distribution of spectra measured in the nonresonant gas under study to the spectra measured in argon and oxygen, respectively. The two nonresonant spectra of each measurement cycle were obtained within a few minutes to avoid de-adjustements caused by long-time drifts. Before each measurement, the cell was flushed and evacuated several times. Because of the much higher threshold for laser-induced breakdown in oxygen compared to argon, first χ_{NR} of oxygen was calibrated carefully (at lower pump and Stokes energies) to be 0.81 ± 0.10 times χ_{NR} of argon (literature value: 0.839). Measurements of this ratio at 437 nm and 473 nm showed no difference. For subsequent measurements oxygen was used as a standard.

In the results reported a possible enhancement of χ_{NR} cancels out, in contrast to a calibration procedure using resonant intensities [20]. In addition, the weak dispersion of χ_{NR} [21] also cancels. The results presented were obtained by USED CARS (either correlated or decorrelated) and by BOXCARS. Each spectrum was the average over 500 individual laser pulses. The spectral shapes of measurement and calibration spectrum were compared in order to detect resonant contributions. However, for the species listed in Table 1, such a resonant contribution was not observed. For the hydrocarbons it should be mentioned that far off-resonant Raman contributions were probably detected. The results of all measurements are summarized in Table 1. For comparison, literature data of nonresonant (electronic) third-order susceptibilities are also listed. All values are scaled to the χ_{NR} of argon measured by the same method. Inspection of Table 1 shows differences in the χ_{NR} of hydrogen and nitrogen from the literature data. This is especially important in air-fed combustion, where nitrogen is the major constituent of the gas. For the hydrocarbons, an increase of χ_{NR} with the numbers of C–H bonds was found; however no linear relation [22] was obtained. The ratio of $\chi_{NR}(H_2)$ to $\chi_{NR}(D_2)$ was measured to be 0.9 which is close to the ratio obtained in [21].

Table 1

Species	Effective χ_{NR} expressed in units of χ_{NR} of Ar [9.6×10^{-18} cm^3/erg]	Literature values
O_2	0.81[e,f]	0.798[3,a], 0.839[1,a]
H_2	0.73[e]	0.598[2,a], 0.63[4,b]
D_2	0.82[e,f]	0.839[1,a]
N_2	0.74[e]	0.87[1,a], 0.88[1,d]
NO	1.97[f]	1.97[3,b]
CO_2	0.96[f]	0.94[3,b]
CH_4	3.31[e]	2.77[3,b]
C_2H_4	8.84[e]	6.36[3,b]
C_3H_6	13.2[e]	–
C_4H_8	15.4[e]	–
i-C_4H_{10}	13.6[e]	12.7 (n-C_4H_{10})[1,c]
SF_6	1.55[e,f]	1.61[1,a], 1.34[1,b]

[a] Ref. [27], [b] Ref. [20], [c] Ref. [7a], [d] Ref. [7b], [e] measured at 473 nm, [f] measured at 437 nm, estimated error bounds of experimental data are ±10%, methods: 1 = CARS, 2 = FISHG, 3 = dcSHG, 4 = THG

The effect of non-Gaussian pump beam fluctuations leads to an increase of ε. In Fig. 3a, two spectra measured in the *identical* mixture of 1 Torr hydrogen and 799 Torr nitrogen with USED CARS are plotted. Shown are the $Q(2)-Q(0)$ transitions of hydrogen. The spectra are normalized to have the same nonresonant signal intensity at a Raman shift of 4175 cm^{-1}. The straight line denotes the spectrum measured with nearly decorrelated pump fields, the dashed line the spectrum with totally correlated pump fields. The decorrelation of the pump fields in USED CARS was achieved by inserting two quartz rods of 50 mm length parallel to the beam in such a way that each covers an opposite $\pi/2$ section of the circular pump beam. From phase-matching requirements it can be calculated that for the pump beam diameter given, two pump photons were used, which differ by 82 degrees within the angular pump beam. Therefore a small amount of correlated signal contribution still remains. Nevertheless a nearly two-fold reduction of resonant intensity is obvious for correlated fields from Fig. 3a. Figure 3b shows spectra measured by BOXCARS and decorre-

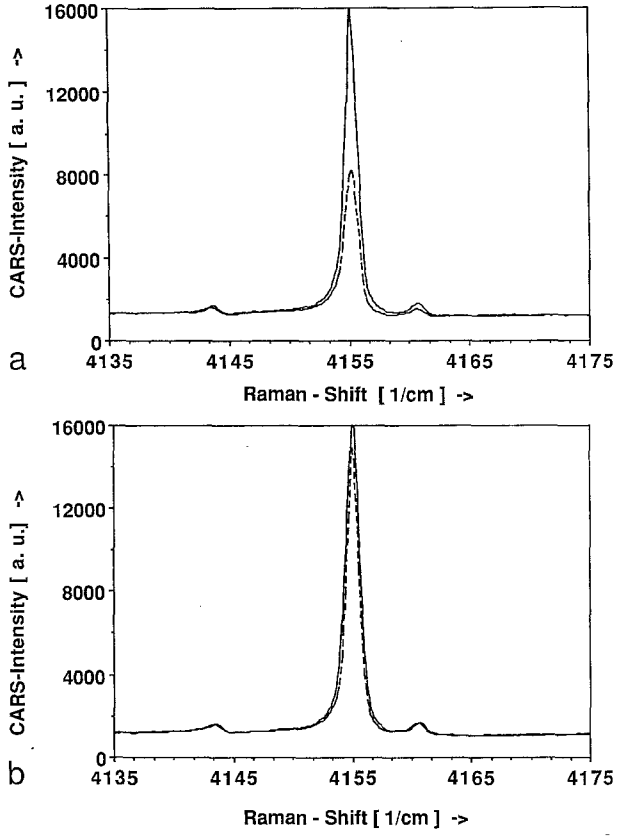

Fig. 3. a USED CARS spectra of 1 Torr hydrogen in nitrogen at 800 Torr measured by correlated pump fields (- - - - -) and nearly decorrelated pump fields (——). **b** Comparison of CARS spectra of 1 Torr hydrogen in nitrogen at 800 Torr measured by BOXCARS (——) and decorrelated USED CARS (- - - - -)

lated USED CARS for the same conditions. As mentioned above, the difference in resonant intensities shown in Fig. 3b is due to the small contribution of correlated signal in USED CARS.

In addition, we have measured the ratio of resonant to nonresonant susceptibilities independently in pure gases. The $Q(1)$-line of hydrogen at 10 Torr served as the resonant signal and 800 Torr of nitrogen as the nonresonant. Assuming an exact square dependence on concentration of the nonresonant signal-intensities, their strength at 10 Torr pressure was calculated. The ratio of resonant hydrogen to nonresonant nitrogen intensities at 10 Torr in correlated USED CARS was found to be $(2.5 \pm 0.3) \times 10^6$, whereas in BOXCARS measurements a ratio of $(4.7 \pm 0.3) \times 10^6$ was obtained. The error bounds describe one standard deviation derived from repeated measurements. From these measurements a ratio ε of 1.9 ± 0.3 is obtained.

The same type of measurements were performed for nitrogen/oxygen. Because nitrogen is most frequently used for CARS-thermometry, its nonresonant third-order susceptibility, Raman cross section and linewidth data have been extensively measured [7, 12, 23]. Figure 4 shows the BOXCARS Q-branch spectrum (straight line) and the USED CARS spectrum obtained with correlated pump fields (dotted-dashed line) both measured in a mixture of 10 Torr nitrogen and 790 Torr oxygen and a theoretical calculation (dashed line) using (1)–(3) and the nonresonant susceptibilities listed in Table 1, respectively. The Raman cross section as recommended in [23] was used and computed for our wavelength. Nitrogen–nitrogen collisions were assumed because of the lack of nitrogen–oxygen collision broadened linewidths. From Fig. 4 it is evident that – similar to the hydrogen case shown in Fig. 3 – an enhancement of χ_{NR} at zero delay occurs. The enhancement was measured in pure gases by the procedure described above at a pressure of 8 Torr. A resonant to nonresonant signal intensity ratio of $(3.3 \pm 0.3) \times 10^4$ was obtained for correlated pump fields in USED CARS, whereas $(8.2 \pm 0.5) \times 10^4$ was determined in BOXCARS. From this the nitrogen Q-branch ratio ε amounts to 2.5 ± 0.3.

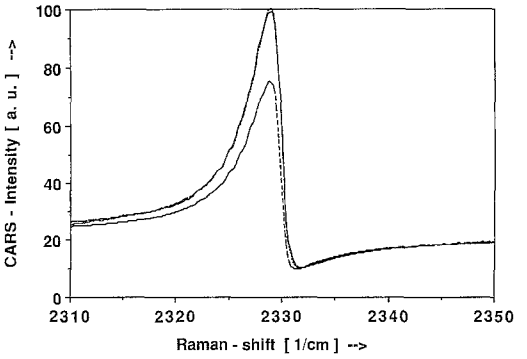

Fig. 4. CARS spectra of 10 Torr nitrogen in oxygen at 800 Torr measured with BOXCARS (——) and correlated USED CARS (· · · · · ·). The dashed line shows the theoretical calculation for the given conditions

Comparing the enhancement of hydrogen and nitrogen we observe for both molecules a behaviour departing from Gaussian pump laser statistics. For pump laser fields with Gaussian statistics ε would be close to 1 for both molecules since the relaxation times at pressures of 10 and 8 Torr, respectively, are much greater than τ_c (12 ps). From the theory outlined in [16] we expect, for a doubling efficiency of 35%, the nonresonant intensity at zero delay to increase by a factor of 3.4, which is higher than the increase obtained in this work. However, on amplifying the fundamental pump field at 1.064 μm a sub-Gaussian field statistics may be created, which reduces the enhancement. Furthermore, the question of Stokes laser statistics is not addressed at all, although it is known [24] that the temporal behaviour of a Stokes dye laser pumped by part of the frequency doubled Nd:YAG laser light roughly follows that of the pump source. In addition, the fact that the nitrogen Q-branch consists of many

overlapping lines might explain the different enhancements observed [14]. Another explanation for different enhancements might be a saturation of the CARS-process. However, as shown in Fig. 3b for H_2 and in Fig. 4 for N_2, spectra measured with decorrelated USED CARS and BOXCARS are similar to each other, although the focal intensities (for the same energies applied) are quiet different. From this we conclude that saturation effects are not significant for our experimental conditions.

There is also evidence of an influence of pump laser field statistics on the shape of the resonant nitrogen Q-branch [14] which is of special interest in CARS thermometry. In simultaneous measurements of temperature and multiple species concentrations [25, 26] the observed enhancement of χ_{NR}/χ_R at zero delay will result in erroneous mole fractions although the spectral fit matches the experimental spectrum.

If one is only interested in measuring the temperature by CARS in flames and plasmas, the best approach, from our point of view, is to allow the nonresonant signal contribution to vary during the regression, i.e. to treat χ_{NR} as a fit parameter as discussed in [22]. This was confirmed by fitting computer generated spectra. The test spectrum was calculated for a 15% mixture of nitrogen in a gas of $\chi_{NR} = 30 \times 10^{-18}\,\mathrm{cm}^3/\mathrm{erg}$ and a temperature of 2000 K.

The initial guess of temperature, mole fraction and χ_{NR} were 1600 K, 30% and $15 \times 10^{-18}\,\mathrm{cm}^3/\mathrm{erg}$, respectively. Other instrumental parameters, except laser linewidth (narrowed by an etalon to $0.2\,\mathrm{cm}^{-1}$), correspond to our experimental setup. Temperature and nonresonant susceptibility were allowed to vary simultaneously for best fit. It was found that five iterations were sufficient to reach a convergence at a fitted temperature of 2000 K. The fitted spectrum could not be distinguished from the computer generated test spectrum. As expected, the fitted nonresonant susceptibility is somewhat greater than twice the χ_{NR} of the test spectrum (the difference is due to the nonresonant susceptibility of nitrogen, which is proportional to the lower nitrogen mole fraction [22]). It can readily be shown that in the weak signal limit, spectra of equal ratio χ_R/χ_{NR} have the same spectral shape [1, 22] and will therefore result in identical fit temperatures. However, due to the collisional linewidth contribution of the diluent gas in environments of low nitrogen mole fraction and at high pressure, it is important to know both the gas composition and its total χ_{NR}.

In conclusion, it has been shown that broadband USED CARS measurements performed with multimode correlated pump fields may result in erroneous mole fractions when fitting the concentration-sensitive shape of CARS spectra generated with non-Gaussian pump laser fields. It is demonstrated that pump fields in USED CARS can be decorrelated to a good approximation in order to minimize the nonresonant signal contribution. The enhancements of hydrogen and nitrogen were shown to differ for reasons not yet well understood. In addition, the effective nonresonant third-order susceptibilities for a number of gases currently used in combustion diagnostics were calibrated at two anti-Stokes wavelengths to that of argon.

Acknowledgements. We gratefully acknowledge helpful discussions with Th. Bouché and financial support of the Stiftung Volkswagenwerk (Grant nr.: I/63394). The authors thank P. Monkhouse for proof reading the translated manuscript.

References

1. A.C. Eckbreth: *Laser Diagnostics for Combustion Temperature and Species* (Abacus Press, Tunbridge Wells 1988)
2. F.Y. Yueh, E.J. Beiting: Appl. Opt. **15**, 3233 (1988)
3. A.C. Eckbreth, T.J. Anderson, G.M. Dobbs: Appl. Phys. B **45**, 215 (1988)
4. R.J. Hall, J.F. Verdieck, A.C. Eckbreth: Opt. Commun. **35**, 69 (1980)
5. H. Kataoka, S. Maeda, C. Hirose: Appl. Spectrosc. **36**, 565 (1982)
6. R.E. Teets: Opt. Lett. **9**, 226 (1984)
7. L.A. Rahn, R.L. Farrow, R.P. Lucht: Opt. Lett. **6**, 223 (1984) R.L. Farrow, L.A. Rahn: J. Opt. Soc. Am. B **2**, 903 (1985)
8. Th. Bouché, Th. Dreier, B. Lange, J. Wolfrum, E.U. Franck, W. Schilling: Appl. Phys. B **50**, 527 (1990)
9. B. Lange, M. Noda, G. Marowsky: Appl. Phys. B **49**, 33 (1989)
10. D.A. Greenhalgh, R.J. Hall: Opt. Commun. **57**, 125 (1986)
11. R.L. Farrow, R.P. Lucht, L.A. Rahn: J. Opt. Soc. Am. B **8**, 1241 (1987)
12. R.L. Farrow, R. Trebino, R.E. Palmer: Appl. Opt. **26**, 381 (1987)
13. M.L. Koszykowski, R.L. Farrow, R.E. Palmer: Opt. Lett. **10**, 478 (1985)
14. G.S. Agarwal, R.L. Farrow: J. Opt. Soc. Am. B **11**, 1596 (1986)
15. A.M.F. Lau, R.L. Farrow: Opt. Lett. **7**, 367 (1989)
16. R.J. Hall: Opt. Commun. **2**, 127 (1985)
17. R.J. Hall: Opt. Quantum Electron. **18**, 319 (1986)
18. E. Dießel, T. Dreier, B. Lange, J. Wolfrum: Appl. Phys. B **50**, 39 (1990)
19. A. Gierulski, M. Noda, T. Yamamoto, G. Marowsky, A. Slenzcka: Opt. Lett. **12**, 608 (1987)
20. T. Lundeen, Shih-Yue, J.W. Nibler: J. Chem. Phys. **79**, 6301 (1983) and references therein
21. V. Mizrahi, D.P. Shelton: Phys. Rev. A **32**, 3454 (1985)
22. R.J. Hall, L.R. Boedecker: Appl. Opt. **23**, 1340 (1984)
23. H.W. Schrötter, H.W. Klöckner: In *Raman Spectroscopy of Gases and Liquids*, ed. by A. Weber (Springer, New York 1979) pp. 123–201
24. D.R. Snelling, R.A. Sawchuk, R.E. Mueller: Appl. Opt. **24**, 2771 (1985)
25. K.W. Boyack, P.O. Hedaman: Fall Meeting of Western States Section, The Combustion Institute, paper-Nr. WSS/CI 89-50 (1989)
26. K. Aron, L.E. Harris, J. Fendell: Appl. Opt. **22**, 3604 (1983)
27. G.J. Rosasco, W.S. Hurst: Phys. Rev. A **32**, 281 (1985)